Water Research 224 (2022) 119067

Contents lists available at ScienceDirect

Water Research

journal homepage: www.elsevier.com/locate/watres

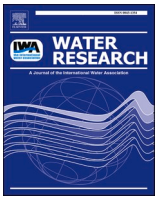

From macrophyte to algae: Differentiated dominant processes for internal phosphorus release induced by suspended particulate matter deposition

Cheng Liu *, Yiheng Du, Jicheng Zhong, Lei Zhang, Wei Huang, Chao Han, Kaining Chen, Xiaozhi Gu

State Key Laboratory of Lake Science and Environment, Nanjing Institute of Geography and Limnology, Chinese Academy of Sciences, No. 73 East Beijing Road, Nanjing 210008, China

ARTICLE INFO

Keywords:
Suspended particulate matter
Internal phosphorus loading
Macrophyte-dominated area
Algae-dominated area
Sediment-water interface
Lake Taihu

ABSTRACT

In shallow lakes, eutrophication leads to a shift of the macrophyte-dominated clear state towards an algae-dominated turbid state. Phosphorus (P) is a crucial element during this shift and is usually concentrated in the suspended particulate matter (SPM) in water. However, the dominant processes controlling internal P release in the algae- (ADA) and macrophyte-dominated (MDA) areas under the influence of P-concentrated SPM remains unclear. In this study, we conducted monthly field observations of P exchange across the sediment-water interface (SWI) with the deposition of SPM in the ADA and MDA of Lake Taihu. Results revealed that both algae- and macrophyte-originated SPM led to the depletion of oxygen across the SWI during summer and autumn. Redox-sensitive P (Fe-P) and organic P (Org-P) were the dominant mobile P fractions in both areas. High fluxes of P across the SWI were observed in both areas during the summer and autumn. However, the processes controlling P release were quite different. In MDA, P release was mostly controlled by a traditional Fe-P dissolution process influenced by the coupled cycling of iron, sulfur, and P. In the ADA, Org-P control was intensified with the deterioration of algal bloom status, accompanied with the dissolution of Fe-P. Evidence from the current study revealed that the dominant process controlling the internal P release might gradually shift from Fe-P to a coupled process of Fe-P and Org-P with the shift of the macrophyte- to an algae-dominated state in shallow eutrophic lakes. The differentiated processes in the MDA and ADA should be given more attention during future research and management of internal P loadings in eutrophic lakes.

1. Introduction

Harmful algal blooms and loss of aquatic vegetation are typical ecological disasters faced by numerous lakes worldwide (Ho et al., 2019; Zhang et al., 2017). The increased algal blooms and decrease of macrophytes result in the shift of a clear state dominated by macrophytes to a turbid state dominated by algae, which is considered a key process in the evolution of eutrophic shallow lakes (Scheffer and Van Nes, 2007). Several factors facilitate such alternative regimes, including climate, nutrients, water depth, and lake size (Coops et al., 2003; Scheffer and Van Nes, 2007). Among these, nutrients have attracted widespread attention owing to their limited availability and assimilation to algae and macrophytes (Andersen et al., 2020). Nitrogen (N) and phosphorus (P) are major concerns subject to debate for decades, with some researchers describing algal growth as limited by both (Conley et al., 2009; Cotner, 2017). Others believe that P or the N/P ratio is more important than N (Qin et al., 2020; Schindler et al., 2016). Regardless, P is established as a crucial element in this context.

Owing to its sedimentation characteristics, P is usually concentrated in suspended particulate matter (SPM) and sediments (Ji et al., 2022; Liu et al., 2019a). Concentrated P is deposited in the sediment through the deposition of SPM, then mobilized and released to the overlying water again through diffusion, resuspension, and other diagenetic processes (Taguchi et al., 2020). Persistent internal P release might increase P concentrations and promote algal blooms even after the reduction of external loads (Nürnberg et al., 2012). During these sedimentation, dissolution, and release processes, the composition and transformation of P fractions are essential. Sedimentary P is commonly divided into loosely adsorbed P (Ex-P), redox-sensitive P (Fe-P), aluminum-bound P (Al-P), organic P (Org-P), apatite, other inorganic P (Ca-P), and residual P (Res-P) (Lukkari et al., 2007). Among these fractions, Ex-P, Fe-P, and Org-P are considered more mobile (Rydin, 2000). The dissolution of

* Corresponding author.
E-mail address: chliu@niglas.ac.cn (C. Liu).

https://doi.org/10.1016/j.watres.2022.119067
Received 22 May 2022; Received in revised form 31 August 2022; Accepted 5 September 2022
Available online 7 September 2022

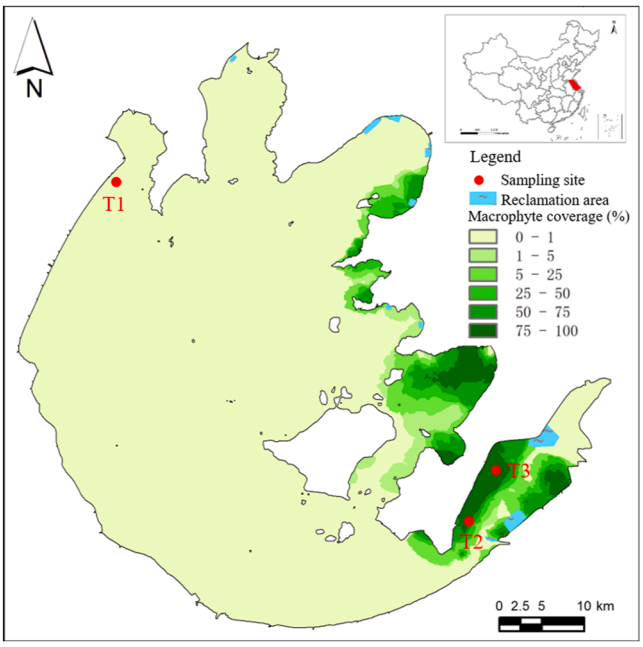

Fig. 1. Locations of the sampling sites and macrophyte distribution in Lake Taihu.

these forms of P has been widely accepted to control P release across the sediment-water interface (SWI).

Previous studies revealed that most of the P in water is present in particulate form (Shinohara et al., 2016), especially in some eutrophic areas where the particulate P (Par-P) ratio can reach 90% or higher (Zhu et al., 2020). The P-concentrated SPM in the algae-dominated area (ADA) was rich in both Fe-P and Org-P (Liu et al., 2019a; Yang et al., 2020). In the macrophyte-dominated area (MDA), a large portion of the P pool was discovered to be in the SPM originated from calcite crusts on macrophytes (Sand-Jensen et al., 2021; Wang et al., 2022). Such P-concentrated SPM aggravates P release from the sediment in both areas (Liu et al., 2019a; Zhao et al., 2019). The differential distribution of P fractions in SPM and the sediment increased the complexity of P exchange across the SWI in the two areas. The dissolution of Fe-P under anoxic conditions has been widely accepted as a typical means for internal P release (Hupfer and Lewandowski, 2008). However, greater dissolution of Fe-P under aerobic conditions was discovered in MDA than in ADA (Kisand and Nõges, 2003). In addition, a series of recent studies have revealed that Org-P is another key factor that controls the release of P, especially in eutrophic shallow lakes with serious algal blooms (Alam et al., 2020; Song et al., 2018). Therefore, there may be different processes that control P release in these two areas.

As an essential element for eutrophication and algal blooms, P release in both the ADA and MDA influences the cycle of P throughout the whole lake. However, information on the differences of dominant processes for P release between these two areas remains limited. Further, whether a shift in the dominant processes controlling P release also occurs during the two states remains unclear. In the current study, monthly field observations of the deposited SPM and P exchanges across the SWI in both the ADA and MDA were carried out in Lake Taihu. The influence of P exchange by deposited SPM originating from the two areas was studied. We sought to reveal the distinct and dominant processes for internal P release in the ADA and MDA of eutrophic lakes.

2. Materials and methods

2.1. Study site and field sampling of the water, sediment, and SPM

Lake Taihu is a typical large shallow eutrophic lake with an area of 2338 km^2 and a mean depth of 2 m. An increase in algal blooms and loss of macrophytes has affected the lake for decades. The maximum algal bloom coverage was reported at 1208 km^2 (Duan et al., 2015). Meanwhile, macrophyte coverage has reduced to only 10.6% of the lake area (Fig. 1). In the past five years, the total phosphorus (TP) concentration in water has continuously increased, with 70% being Par-P (Zhu et al., 2020). Field observations were carried out monthly from May 2018 to April 2019 for both the ADA (T1) and MDA (T2 and T3). The bloomed algae in the ADA were mostly cyanobacteria Microcystis spp. (Qin et al., 2019). The dominant macrophytes in the MDA were *Potamogetom crispus* in spring and *Potamogeton malaianus, Vallisneria natans, Hydrilla verticillata, Potamogeton pectinatus, Trapa bispinosa*, and *Myriophyllum spicatum* in summer according to our field observation and other studies (Zhang et al., 2022). During each sampling period, three sediment cores were collected from each site using a gravity corer (90 mm diameter, 500 mm length; Rigo Co., Ltd., Japan). Approximately 1 L of lake water from each site was simultaneously sampled. All the sediment columns and water samples were preserved at 4 °C, transported to the laboratory within 3 h, and then analyzed immediately. In parallel to the sampling of water and sediment columns, deposited SPM at each site was also collected using self-designed sediment traps. Each trap had 16 channels of plexiglass tubes (90 mm diameter, 500 mm length). On each sampling period, two sets of traps were deployed at each sites in Fig. 1. Details of the SPM collection are described in the Supplementary Material. SPM from the same site was homogenized, preserved at 4 °C, and immediately transported to the laboratory for analysis. For each site, the sedimentation rate of SPM was calculated by freeze drying the fresh SPM in three tubes to a constant weight under vacuum conditions.

2.2. Profile analysis and calculation

Immediately after the sediment columns were transported to the laboratory, the vertical profiles of oxygen (O_2) across the SWI were analyzed using a micro-profiling system (Unisense, Aarhus, Denmark). Thereafter, the pore water profiles of soluble reactive P (SRP) and ferrous iron (Fe(II)) were obtained using a series of mini-peepers (Fig. S1). After obtaining the profile characteristics, the O_2 uptake rate was calculated based on Fick's second law assuming zero-order kinetics (Rasmussen and Jorgensen, 1992). The diffusive fluxes of SRP and Fe(II) across the SWI were calculated using Fick's first law of diffusion (Ullman and Aller, 1982). The details of profile analysis and calculation are provided in the Supplementary Material.

2.3. Chemical analysis

The total suspended solids, TP, total dissolved P, SRP, Par-P, organic P (Org-P), and chlorophyll a (Chla) concentrations in water were analyzed. The sediment columns were segmented at 2-cm intervals. The sediment and SPM samples were analyzed for reduced inorganic sulfur fractions (acid volatile sulfide, Cr(II)-reducible sulfur, and elemental sulfur), P fractions, typical metals that usually precipitate with P (aluminum (Al), iron (Fe), and calcium (Ca)), and total organic carbon (TOC). The details of these chemical analyses are described in the Supplementary Material.

2.4. Statistical analysis

Pearson's or Spearman's correlations between various characteristics in the sediment and SPM were analyzed. The differences of various characters between different sites and times were evaluated using paired *t*-test or one-way analysis of variance (ANOVA) tests. Significance was reported at $p < 0.05$ and $p < 0.01$ levels. These tests were carried out using SPSS software (version 26.0; IBM, New York, NY, USA). Correlation plots and other data figures were generated using Origin software (version 2021; OriginLab, Northampton, MA, USA).

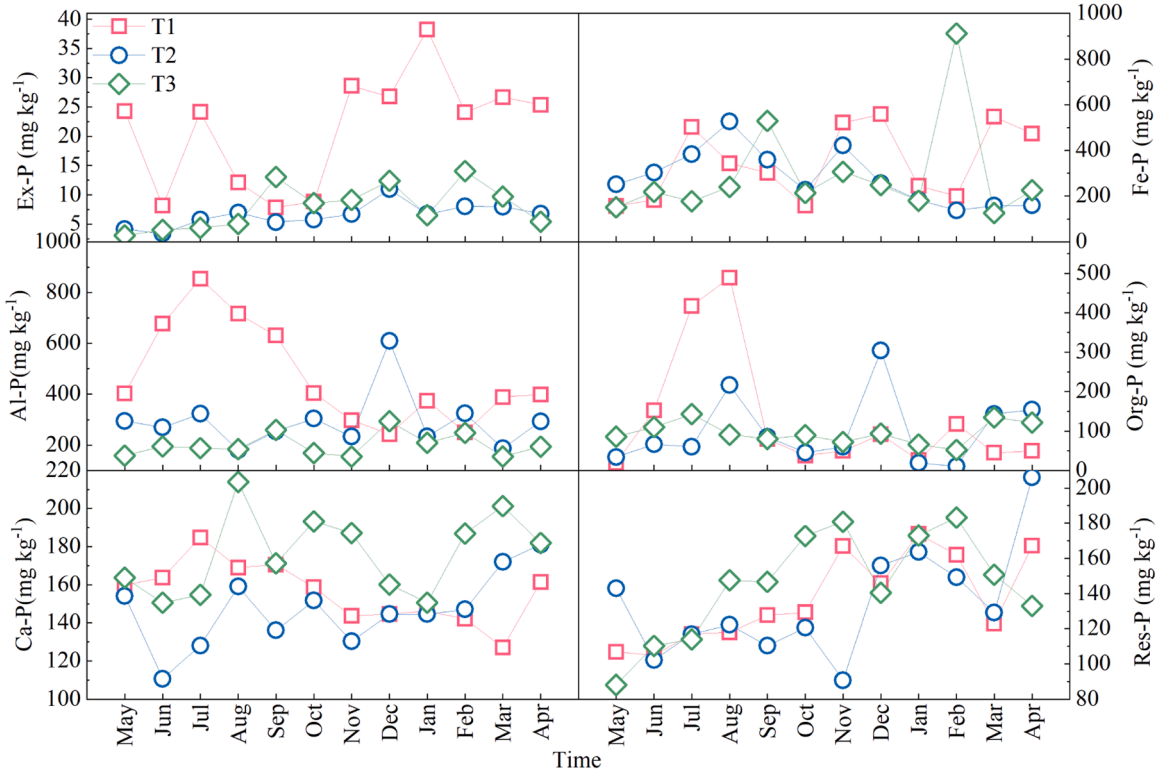

Fig. 2. Monthly variations of phosphorus fractions in suspended particulate matter.

3. Results

3.1. Monthly water quality variations in the algae- and macrophyte-dominated areas

Water TP, SRP, Par-P, and Org-P concentrations in the ADA were generally higher than those in the MDA throughout most of the study period (Fig. S2). TP concentrations in T1 reached a peak of 0.70 mg L^{-1} in August, accompanied by high SRP (0.18 mg L^{-1}), Par-P (0.52 mg L^{-1}), total dissolved P (0.19 mg L^{-1}), Chla (228.1 μg L^{-1}), and total suspended solids (84.0 mg L^{-1}) concentrations. Two small peaks in TP concentrations in T2 and T3 occurred in June (0.09 mg L^{-1}) and February (0.09 mg L^{-1}), respectively. The dominant P fraction in the water of both areas was Par-P, with the highest ratios of 86% and 94% for ADA and MDA, respectively. While the Par-P concentrations in the ADA were much higher than those in the MDA, especially during summer. For the ADA, Par-P and other fractions of P in the water were considerably higher in summer as was Chla concentration. Significantly positive correlation (Pearson's $r = 0.935$, $p < 0.01$) was discovered between the Par-P and Chla in water. For the MDA, no significant correlations were discovered between the Par-P and Chla.

3.2. Properties of the deposited SPM

3.2.1. Development of sedimentation rate of the SPM

The sedimentation rate in ADA was much higher than that in MDA throughout the investigation (Fig. S3(a), $p < 0.01$, ANOVA). The highest sedimentation rate of 978.8 g dw m^{-2} d^{-1} for T1 was observed in September, close to that in August. After April, the sedimentation rate of T1 increased dramatically and was significantly positively correlated with Chla in water (Pearson's $r = 0.580$, $p < 0.01$). The trends of sedimentation rate were quite similar between T2 and T3 ($p = 0.122$, paired *t*-test), with two increase periods in spring and early winter, when the withering of *Potamogetom crispus and other submerged macrophytes occurred, respectively.* These trends indicated that the sedimentation rate in T1 might be related to the algal bloom, whereas that in T2 and T3 might be related to macrophyte withering.

3.2.2. TOC contents in the SPM

The TOC content of T1 was significantly lower than of T2 and T3 (Fig. S3(b), $p < 0.01$, ANOVA). The highest TOC (5.90%) in T1 was recorded in July, when a serious algal bloom occurred. The TOC for T2 and T3 ($p = 0.677$, paired *t*-test) increased from March to September, gradually decreasing from September to February. During the high macrophyte growing and withering seasons (July to January), the TOC of T2 and T3 were both higher than 5%, peaking at 6.42% and 6.87%, respectively. The TOC of T1 was significantly positively correlated with Chla ($p < 0.01$, Fig. S4(a)). The TOC of T2 and T3 was negatively correlated with Chla, yet not significantly (Fig. S4(b)). The bloomed algae at T1 might have had a significant influence on TOC content in the SPM, while the TOC of T2 and T3 might be influenced by macrophyte.

3.2.3. Phosphorus fractions in the SPM

Generally, TP concentrations in the SPM of T1 were higher than those of T2 and T3 (Fig. 2, $p < 0.01$, ANOVA). The Ex-P concentrations of T1 were higher than those of T2 and T3 at most times throughout the year. Ex-P was much lower than the other P fractions for all sites. Fe-P and Org-P were the dominant mobile P fractions. The Fe-P concentrations of T1 were close to those of T2 and T3, whereas the Org-P of T1 increased dramatically after May and peaked in August, at 489.2 mg kg^{-1}. The trend was consistent with Chla increase during this period (Fig. S2). In the other months, the Org-P of T1 was similar to that of T2 and T3. Al-P and Ca-P were also the dominant fractions of inorganic P in SPM. The ratios of Ca-P to TP for T2 and T3 were higher than those of T1.

3.2.4. Typical metals in the SPM

As per Section 3.2.3, Fe-P, Al-P, and Ca-P represented key fractions of inorganic P in the SPM. Fe ($p = 0.037$) and Al ($p < 0.01$, ANOVA) concentrations of T1 were slightly higher than those of T2 and T3, particularly in autumn and winter (Fig. S5). The Fe and Al concentration

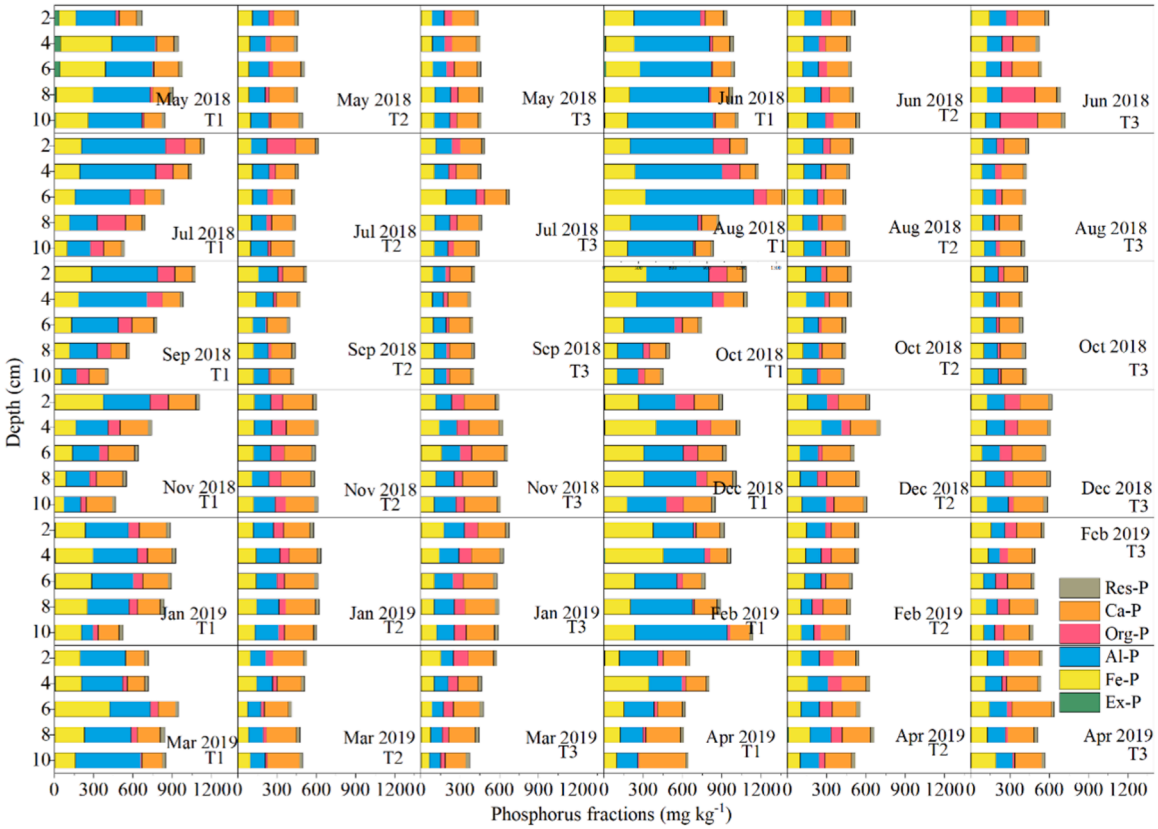

Fig. 3. Vertical distributions of phosphorus fractions in the sediment.

of T1 were relatively stable, while decreased obviously for T2 and T3 from summer to winter. The Ca concentration of T1 was also quite stable throughout and obviously lower than for T2 and T3 ($p < 0.01$, ANOVA, Fig. S5).

3.3. Properties of the sediment columns

3.3.1. Vertical distributions of TOC in the sediment columns

TOC concentrations in the sediment columns of all three sites were lower than those in the SPM of corresponding sites (Section 3.2.2), especially T2 and T3. The TOC concentration in the sediment of T1 was significantly lower than that of T2 and T3 ($p < 0.01$, ANOVA), similar to that of SPM (Fig. S6). The TOC in the surficial 2 cm sediment of T1 experienced a slight increase in July and August, which might have been caused by the significant increase in TOC in the SPM during this period (Section 3.2.2). There was no obvious increase in the TOC of T2 and T3 surficial sediments. The influence of the deposited SPM on sediment TOC concentration in ADA was more obvious than for MDA during the serious algal bloom season.

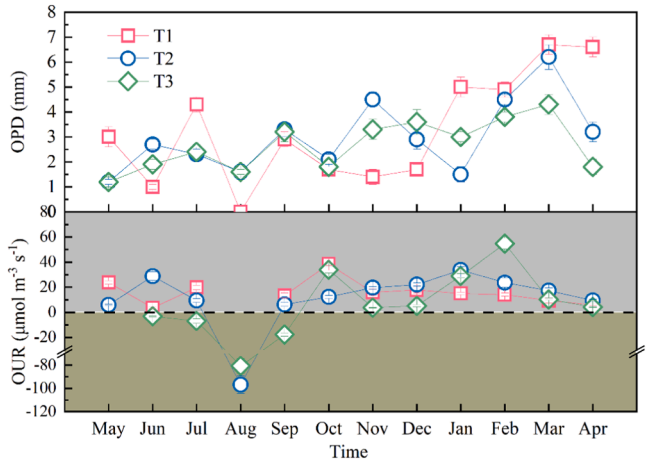

Fig. 4. Oxygen penetration depth (OPD) and oxygen uptake rate (OUR) across the SWI.

3.3.2. Phosphorus fractions in the sediment columns

The TP concentration in the sediment of T1 was higher than those of T2 and T3 ($p < 0.01$, ANOVA, Fig.3), all were lower than those in the SPM. Similar to the P fraction in SPM, Fe-P and Org-P were also the dominant mobile P in the sediment. Ex-P was quite low compared to the other fractions. A significant increase in Org-P in T1 was observed from May to October, especially in the surficial 2 cm of the sediment, with the highest value of 150.8 mg kg^{-1} in July. The increase of P in the MDA mostly occurred in winter, with a slight increase in Fe-P and Org-P. Fe-P concentrations in T2 and T3 remained low during the summer and autumn, when temperatures are highest.

3.3.3. Typical metals in the surficial sediment

The concentrations of Fe and Al in the sediment of T1 were significantly higher than those of T2 and T3 ($p < 0.01$, ANOVA, Fig. S7). The Fe and Al concentrations of T1 increased from December to March and were similar to those in the SPM (Section 3.2.4). Similar to concentrations in the SPM, Ca in the sediment of T1 remained stable and lower than in T2 and T3 ($p = 0.016$, ANOVA). A trend of increase in Ca concentrations was observed for both T2 and T3 from October to January, potentially caused by high levels of Ca in the SPM during this period (Fig. S5).

3.3.4. Reduced inorganic sulfur fractions in the surficial sediment

Acid volatile sulfide and Cr(II)-reducible sulfur were the dominant fractions of reduced inorganic sulfur in the sediments of both ADA and

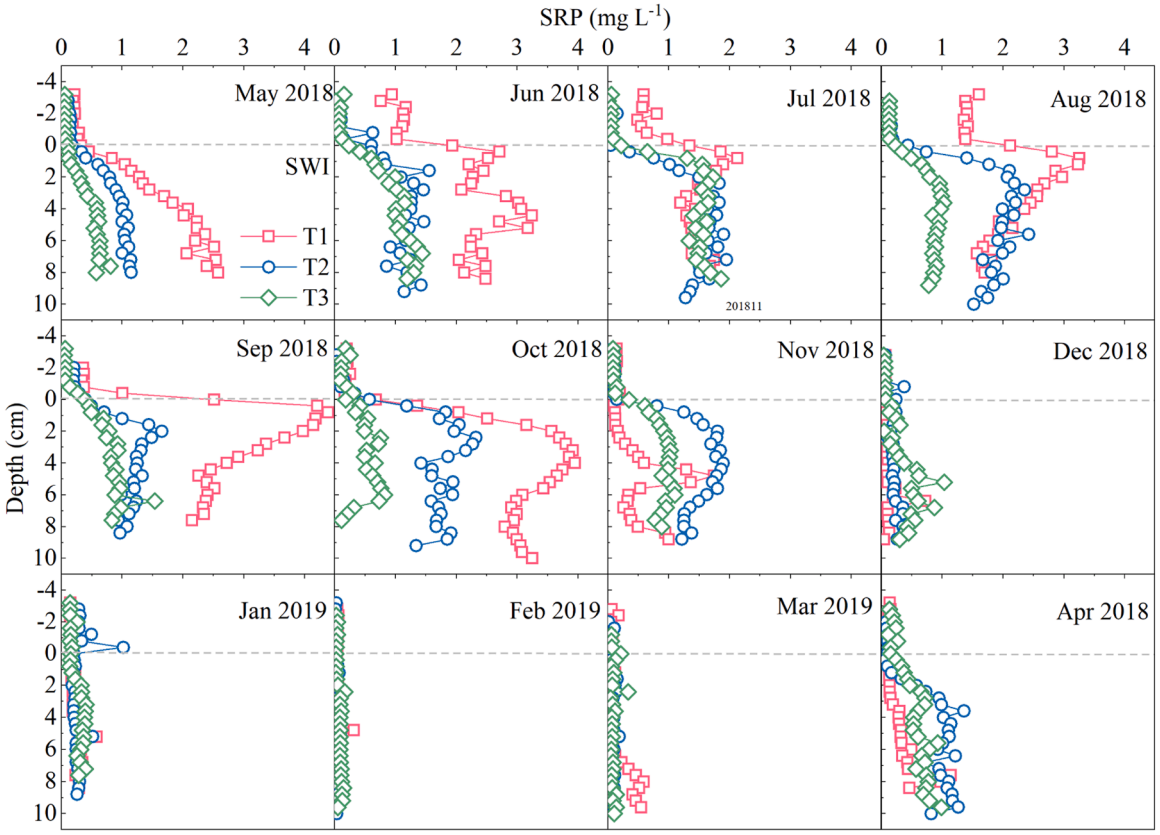

Fig. 5. Soluble reactive phosphorus (SRP) concentrations in the pore water.

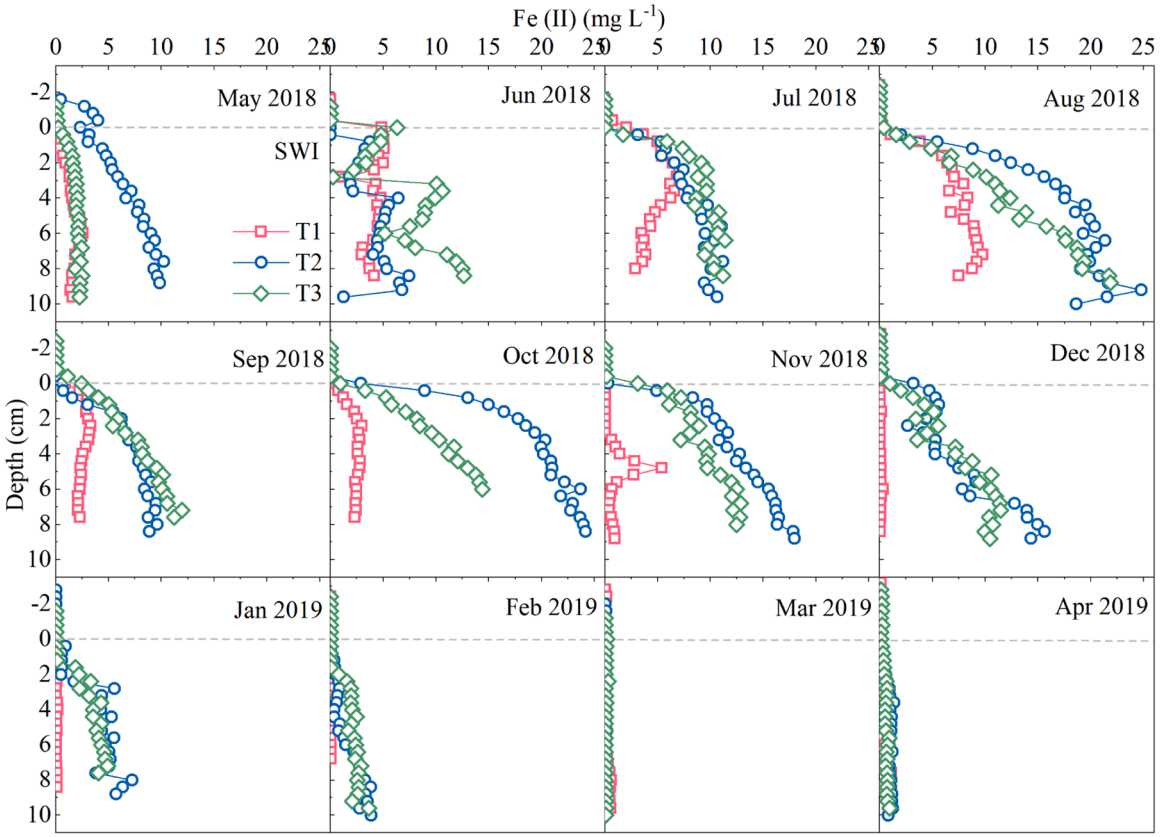

Fig. 6. Ferrous iron (Fe(II)) concentrations in the pore water.

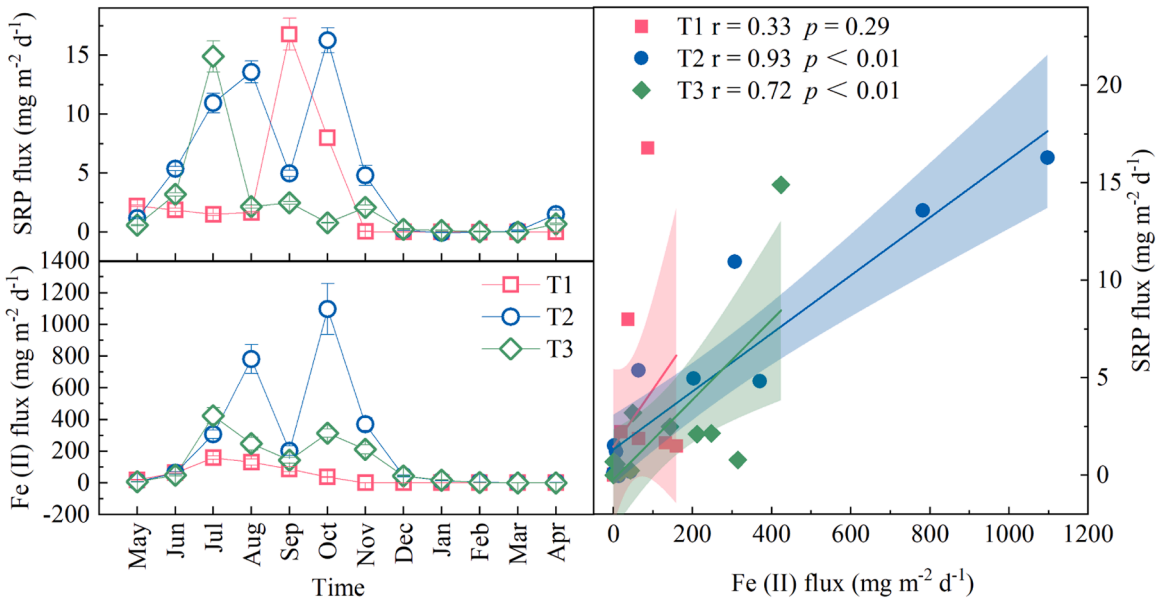

Fig. 7. Fluxes of soluble reactive phosphorus (SRP) and Fe(II) across the sediment-water interface and their correlations.

MDA (Fig. S8). Acid volatile sulfide and Cr(II)-reducible sulfur concentrations in the sediments of T2 and T3 increased from May to September and were significantly higher than those in T1. Generally, the reduced sulfur concentrations in the MDA were higher than those in the ADA during summer and autumn, probably caused by the high TOC (Section 3.3.1) induced sulfate reduction rates in the area (Kim et al., 2017).

3.4. Profile characteristics and fluxes across the SWI

3.4.1. O_2 profiles and uptake rates across the SWI

The O_2 profiles showed significantly differences between different sites and sampling periods ($p < 0.01$, ANOVA, Fig. S9). From May to August, the oxic sediment zone of T1 narrowed gradually (Fig. S9), with the O_2 penetration depth (OPD) decreasing from 3.0 mm to 0 (Fig. 4). An extreme anoxic condition of the SWI was observed in August when O_2 in the bottom water decreased to 0. Significantly negative correlations were discovered between the Chla in water and OPD (Pearson's $r = -0.346$, $p = 0.039$). The OPD remained lower than 2 mm until December. From December to April, the OPD of T1 gradually increased to approximately 7 mm (Fig. 4). O_2 concentrations across the SWI for T2 and T3 were also low from May to August (Fig. S9). However, the OPD of both T2 and T3 ($p = 0.231$, paired *t*-test) exhibited a slow increase from May 2018 to March 2019. The lowest OPD for T2 and T3 were observed from April to May. Notably, negative O_2 uptake rate values for T2 and T3 were detected from June to September, especially in August (Fig. 4), when the highest biomass of submerged macrophytes was recorded (Fig. 1).

3.4.2. Pore water profiles of SRP and Fe(II) across the SWI

The pore water SRP concentrations were generally higher from May to October, with those of T1 being higher than for T2 and T3 ($p < 0.01$, ANOVA, Fig. 5). After November, the SRP concentrations at all three sites decreased sharply, especially for T1. This decrease in SRP at T1 occurred slightly earlier than that at T2 and T3, resulting in lower SRP concentrations in the former site from November to April. The vertical distributions of SRP remained relatively constant from the overlying water to the deeper sediment for all three sites, under the low winter temperatures from December to March.

The Fe(II) concentrations of T1 were relatively higher from May to October (Fig. 6) and were slightly higher than those of SRP during the same period, which did not allow for Fe and P co-precipitation in the oxic sediment zone (Lehtoranta et al., 2009). From November to April, the Fe(II) concentrations of T1 decreased sharply to under 0.5 mg L^{-1} or even close to 0. The concentrations of Fe(II) for T2 and T3 were remarkably higher than those for T1 ($p < 0.01$, ANOVA), which could be noticed during most of the year. In particular, significant increases in Fe (II) for T2 and T3 were observed after September when the temperature began to decline and the Fe(II) of T1 began to decrease. Even in winter (December to February), the Fe(II) concentrations of T2 and T3 were significantly higher than those of T1 and the corresponding SRP concentrations ($p < 0.01$, ANOVA).

3.4.3. Fluxes of SRP and Fe(II) across the SWI

The SRP fluxes of T1 remained stable between 1.50 and 2.23 mg m^{-2} d^{-1} from May to August, which were already within the range of high P fluxes in many eutrophic lakes (Gibbons and Bridgeman, 2020; Nürnberg et al., 2012). The highest SRP fluxes of T1 reached 16.79 mg m^{-2} d^{-1} in September and then decreased quickly. The SRP fluxes of T2 and T3, however, increased gradually after May and peaked in July and August, with fluxes of 14.90 and 13.57 mg m^{-2} d^{-1}, respectively. Similarly, the P fluxes of all three sites decreased sharply after November and remained low until the following April. The Fe(II) fluxes of T1 increased gradually after May and peaked in July at 158.77 mg m^{-2} d^{-1}, decreasing gradually thereafter, down to below 0.2 mg m^{-2} d^{-1} after November. The highest values of T2 and T3 reached 1097.24 and 423.46 mg m^{-2} d^{-1} in October and July, respectively. These values were considerably higher than for T1 and the SRP fluxes at these two sites. Further analysis revealed significant positive relationships between Fe (II) and SRP fluxes in T2 and T3 (both $p < 0.01$), but not in T1 (Fig. 7). The simultaneous release of Fe(II) and SRP in T2 and T3 was more evident than in T1.

4. Discussion

4.1. Deposition of algae- and macrophyte-originated SPM induced differential environmental changes across the SWI

Previous studies have shown that the decomposition of algae and macrophytes could lead to O_2 depletion as well as the release of P and other elements (Liu et al., 2015; Shen et al., 2014). The deposition and decomposition of algae- and macrophyte-derived SPM may play vital roles during these processes. However, the time periods of SPM

deposition were significantly different. The deposition of algae-originated SPM was mostly observed from late spring to autumn with high sedimentation rates (Section 3.2.1), especially in the summer, when Lake Taihu faced the most severe algal bloom (Qin et al., 2019). The algae-derived SPM resulted in high concentrations of TOC in the SPM and the surficial sediment (Sections 3.2.2 and 3.3.1), as well as high levels of protein-like organic matter (Liu et al., 2019a). Consequently, a rapid decomposition process occurs after SPM deposition, especially during summer and autumn with high temperatures (Derrien et al., 2019; Diaz and Rosenberg, 2008). Our previous study in Lake Taihu revealed that the decomposition of algae-originated SPM generally took place within 5 days, and O_2 was depleted within 2 days (Liu et al., 2019b, 2015). In the current study, O_2 across the SWI in the ADA decreased to 0 from May to August and remained at low levels until the end of autumn (Section 3.4.1). The decomposition of algae-originated SPM led to low O_2, low OPD, and a high consumption of O_2 across the SWI.

As shown in Section 3.2.1, the deposition of SPM in the MDA was influenced by the two withering periods of different macrophytes. The withering of *Potamogetom crispus* resulted in a short period of O_2 depletion in late spring, which has also been observed in previous studies (Shen et al., 2014). While in summer, although high TOC in the SPM and sediment of T2 and T3 (Sections 3.2.2 and 3.3.1) might have led to the intense mineralization and consumption of O_2 at high temperatures (Derrien et al., 2019; Li et al., 2018), the depletion of O_2 across the SWI was not as drastic as that of T1. The radial O_2 losses effect usually increases the depth of the oxic sediment zone around the rhizosphere (Han et al., 2018; Koop-Jakobsen et al., 2017). Thus, increased OPD from May to September, and negative O_2 uptake rates were observed in the MDA under high macrophyte coverage (Section 3.4.1). Comparing ADA and MDA, algae-originated SPM led to the sharp depletion of O_2 across the SWI during summer and autumn, while macrophyte-originated SPM mostly led to O_2 depletion in late spring. These environmental changes may further influence P exchange across the SWI (Hupfer and Lewandowski, 2008; Søndergaard et al., 2003).

4.2. Deposited SPM led to discrepant P sedimentation processes in the ADA and MDA

As revealed in Sections 3.2.3 and 3.3.2, Ca-P, Fe-P, and Al-P were the dominant inorganic P fractions in the SPM and sediment. The dominant status of Ca-P in the MDA was more evident than that in the ADA. During the fast growth season, large quantities of calcite crusts can frequently form on the leaves and stems of submerged macrophytes during daytime photosynthesis (Blindow, 1992; Dong et al., 2014; Kisand and Nõges, 2003; Pełechaty et al., 2013; Sand-Jensen et al., 2021). The co-precipitation of Ca and P through calcite crusts resulted in higher ratios of Ca-P in the MDA than in the ADA (Dierberg et al., 2002; Wang et al., 2022). Unlike Ca distribution, the Fe and Al concentrations in the SPM and sediment in the ADA were generally higher than those in the MDA, resulting in high concentrations of Fe-P and Al-P (Section 3.3.2). Among these two fractions, Al-P was considered more stable than Fe-P by many researchers (Rönicke et al., 2021; Rydin, 2000). Aluminum treatment was also considered more efficient over longer time series in many lakes (Rönicke et al., 2021; Yin et al., 2018). Therefore, high concentrations of redox-sensitive Fe-P may be more important for internal P release (Gu et al., 2019; Hupfer and Lewandowski, 2008). An increased Fe/P ratio is usually considered to increase stability of the P pool in the sediment (Jensen et al., 1992). With regard to Fe/P, T2 and T3 were quite close in both SPM ($p = 0.126$, paired t-test) and the sediment ($p = 0.427$, paired t-test), being generally higher than T1 values at most times of the year, especially in summer (Fig. S10(a) and (b)). The Fe/P ratio of the sediment was significantly positively correlated with that of SPM (Pearson's $r = 0.564$, $p < 0.01$, Fig. S10(c)), demonstrating the direct influence of SPM on the sedimentation of Fe and P in surficial sediments. From May to August, Fe/P in both areas decreased sharply, accompanied by a decrease in Fe-P. The obvious decrease in Fe-P at all three sites indicated a potential influence of Fe-P on the internal P cycle in both areas, which has already been described as the dominant process for internal P release in many lakes (Alam et al., 2020; Tammeorg et al., 2020).

As per Section 3.1, the dominant P fraction in the water of both areas was Par-P, whereas the sources of these P-concentrated SPM were different. For the ADA, the bloomed algae were the most likely sources of Par-P in the water and the SPM (Sections 3.1 and 3.2.1). An increase in mobile P in the SPM was also observed with the increase of Par-P in summer (Section 3.2.3). The increase in Org-P in SPM was greater than those of Ex-P and Fe-P. Our previous field observations in the ADA of Lake Taihu also revealed that Org-P was the dominant fraction of P in the algae-originated SPM (Kong et al., 2020). A similar distribution of Org-P in SPM was also discovered in the ADA of Lake Chaohu (Liu et al., 2019a; Yang et al., 2020). The increased Org-P content in the SPM gave rise to Org-P in the surficial sediment in summer (Section 3.3.2), which has also been considered a key factor influencing P release in many eutrophic areas (Amirbahman et al., 2013; Markovic et al., 2019). For MDA, there was no obvious increase of Org-P in the SPM and the surficial sediment during summer. Therefore, the discrepant origins and elemental compositions of SPM led to differential P sedimentation processes in the ADA and MDA, which would further influence the internal P cycle in these two areas.

4.3. Differences of dominant processes for P dissolution and exchange across the SWI in the ADA and MDA

Differential P sedimentation processes caused by deposited SPM in the ADA and MDA resulted in differential distributions of mobile P in the sediment (Section 3.3.2). For both the areas, Fe-P and Org-P were the dominant mobile P fractions. For ADA, the anoxic conditions in summer (Section 3.4.1) induced the dissolution of Fe-P (Hupfer and Lewandowski, 2008). In parallel, the concentrations of SRP and Fe(II) in pore water increased significantly (Section 3.4.2). Fe-P concentration in the sediment was also negatively correlated with temperature and Chla (Fig. S4). Therefore, Fe-P dissolution is believed to occur during the severe algal bloom season at high temperatures, which is consistent with previous studies (Gibbons and Bridgeman, 2020; Hupfer and Lewandowski, 2008). In addition, the mineralization of organic matter would also lead to Org-P dissolution. This process is further enhanced by iron reduction (Markovic et al., 2019). During the algal bloom season, a significant increase in the Org-P difference between SPM and the surficial sediment was observed (Fig. S11). The Org-P difference was significantly higher than the Fe-P difference during this period. In addition, the pore water Fe(II) concentrations in T1 were close to or slightly higher than those of SRP (Section 3.4.2), which did not allow for Fe and P co-precipitation in the oxic sediment zone (Lehtoranta et al., 2009). These phenomena indicate that a large part of the deposited Org-P might have been mineralized and released in the ADA. The subsequent decrease in Org-P and the low OPD after September indicated further mineralization of Org-P in autumn (Markovic et al., 2019). For the MDA, Org-P in the surficial sediment and SPM was significantly lower than in the ADA during summer and autumn (Sections 3.2.3 and 3.3.2). Moreover, the Org-P difference for T2 and T3 was significantly lower than that of T1 ($p < 0.01$, paired t-test) and the Fe-P difference during this period ($p < 0.05$, paired t-test, Fig. S11). The Fe-P differences of T2 and T3 exhibited a general increase from May to September, being mostly higher than that of T1 during summer and autumn. The pore water profiles also showed that Fe(II) concentrations in T2 and T3 were several times the corresponding SRP concentrations from May to December (Section 3.4.2). Therefore, the dissolution of Fe-P in MDA was more obvious than that in ADA.

As discussed in the current section and Section 4.2, Fe-P dissolution during summer and autumn was observed in both areas. However, large differences were noted, as Fe-P dissolution in the MDA was considerably

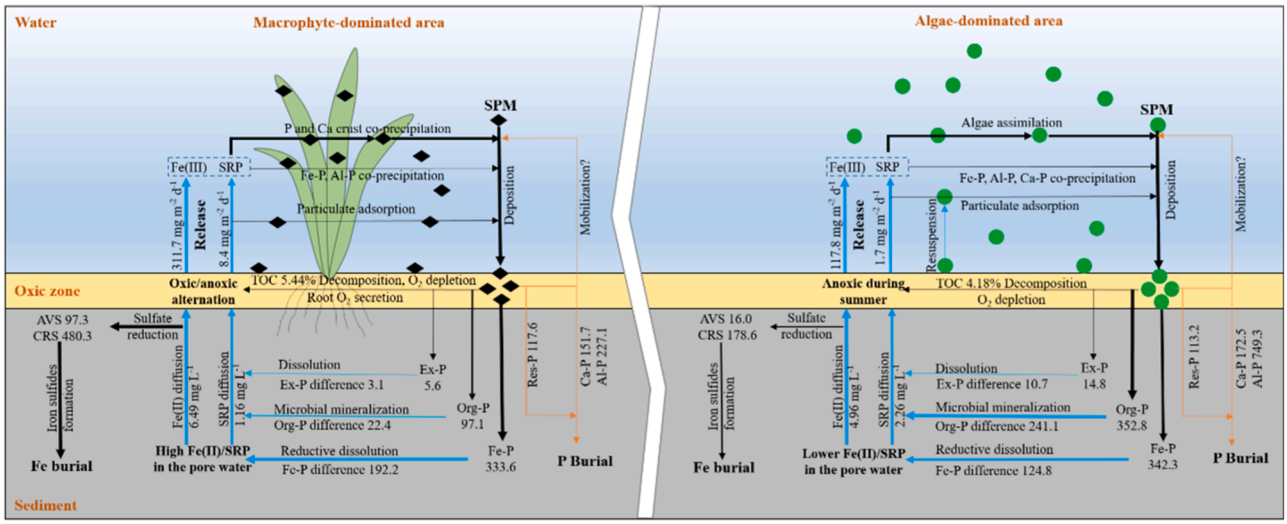

Fig. 8. Dominant processes for P release in the algae- and macrophyte-dominated areas (concentrations and fluxes are the mean values during June 2018 to August 2018 in Lake Taihu. The units of chemicals in the sediment were mg kg^{-1}. Black lines represent precipitation, assimilation, deposition or burial processes. Blue lines represent dissolution, mineralization, resuspension or release processes. SPM: suspended particulate matter; P: phosphorus; Ex-P: loosely adsorbed P; Fe-P: redox sensitive P; Al-P: aluminum-bound P; Org-P: organic P; Ca-P: apatite and other inorganic P; Res-P: residual P; SRP: soluble reactive phosphorus; TOC: total organic carbon; AVS: acid volatile sulfide; CRS: Cr(II)-reducible sulfur).

greater than that of other P fractions. The significant positive relationship between SRP and Fe(II) fluxes ($p < 0.01$) also indicated the simultaneous release of P and Fe(II) (Section 3.4.3). While for the ADA, no significant relationship was discovered between the fluxes of SRP and Fe(II) (Section 3.4.3). The simultaneous dissolution of Fe-P and Org-P during the algal bloom season would both influence the release of P. Consequently, different dominant processes for P release in ADA and MDA were deduced (Fig. 8). P release in the MDA is generally controlled by a traditional Fe-P dissolution process influenced by the coupled cycling of iron, sulfur, and P across the SWI, which has already been described in numerous previous studies (Lehtoranta et al., 2009; Rozan et al., 2002). The high concentrations of reduced sulfur in the MDA (Section 3.3.4) might facilitate the formation of iron sulfides, sequentially restraining the co-precipitation of Fe and P in the oxic sediment layer and enhancing the release of P after Fe-P dissolution (Lehtoranta et al., 2009). Therefore, the SRP fluxes of T2 and T3 were mostly higher than those of T1 during the summer and autumn (Fig. 7). In addition, there are still some other factors that might result in the higher P fluxes in the MDA, including the decaying of macrophyte debris in the sediment (Shen et al., 2014), the lower concentrations of P in the overlying water of the MDA, or the artefact caused by the calculation of fluxes using Fick's first law of diffusion (Ullman and Aller, 1982). These factors influencing the internal P release in the MDA still require further study. With the development of eutrophication and algal blooms, the traditional Fe-P controlled process was shifted to a coupled process controlled by both Fe-P and Org-P in the ADA. Moreover, the control of Org-P might gradually intensify with the deterioration of algal bloom status. A widely accepted phenomenon for the evolution of eutrophic shallow lakes (Scheffer and Van Nes, 2007), the shift between the macrophyte- and algae-dominated status might also shift the dominant processes for internal P release controlled by Fe-P and Org-P. In addition, due to the high Ca-P co-precipitation by the crust on macrophytes (Section 4.2), the sedimentation and dissolution of Ca-P might also play an important role in internal P cycling in the MDA (Dierberg et al., 2002; Kisand and Nõges, 2003; Wang et al., 2022). However, the Ca-P in the sediment was mostly higher than in the SPM. Sedimentation might still be the prevailing process for Ca-P. The dissolution of Ca-P in the MDA or other similar areas with high ratio of Ca-P requires further investigation.

5. Conclusions

A yearlong field investigation in the ADA and MDA of Lake Taihu revealed that both algae- and macrophyte-originated SPM led to the depletion of O_2 across the SWI during summer and autumn. The different characteristics of deposited SPM resulted in differential P sedimentation and release processes in the two areas. A traditional Fe-P dissolution process influenced by the coupled cycling of iron, sulfur, and P was observed in the MDA. With the development of eutrophication and algal blooms, the control of Org-P might be intensified, and a coupled process controlled by both Org-P and Fe-P was discovered in the ADA. Therefore, we further deduced that the dominant process for internal P release might gradually shift from Fe-P to a coupled process of Fe-P and Org-P with the shift of macrophytes to algae in eutrophic shallow lakes. Similar processes might occur in shallow freshwater lakes with the deterioration of eutrophic statuses.

Authors' contributions

Cheng Liu designed the research, wrote the paper, and performed the experiment; Yiheng Du performed the field investigation and laboratory analysis; Jicheng Zhong and Lei Zhang reviewed and edited the paper; Wei Huang and Chao Han participated in the field investigation and edited the paper; Kaining Chen and Xiaozhi Gu supervised the research and reviewed the paper.

Declaration of Competing Interest

The authors declare that they have no known competing financial interests or personal relationships that could have appeared to influence the work reported in this paper.

Acknowledgments

This work was supported by the National Natural Science Foundation of China [grant numbers 42077310, 42177228, and 42177227] and the Young Scientific and Technological Talents Support Project of Jiangsu Province [2020].

Supplementary materials

Supplementary material associated with this article can be found, in the online version, at doi:10.1016/j.watres.2022.119067.

References

Alam, M.S., Barthod, B., Li, J., Liu, H., Zastepa, A., Liu, X., Dittrich, M., 2020. Geochemical controls on internal phosphorus loading in Lake of the Woods. Chem. Geol. 558, 119873.

Amirbahman, A., Lake, B.A., Norton, S.A., 2013. Seasonal phosphorus dynamics in the surficial sediment of two shallow temperate lakes: a solid-phase and pore-water study. Hydrobiologia 701, 65–77.

Andersen, I.M., Williamson, T.J., González, M.J., Vanni, M.J., 2020. Nitrate, ammonium, and phosphorus drive seasonal nutrient limitation of chlorophytes, cyanobacteria, and diatoms in a hyper-eutrophic reservoir. Limnol. Oceanogr. 65, 962–978.

Blindow, I., 1992. Long-and short-term dynamics of submerged macrophytes in two shallow eutrophk lakes. Freshw. Biol. 28, 15–27.

Conley, D.J., Paerl, H.W., Howarth, R.W., Boesch, D.F., Seitzinger, S.P., Havens, K.E., Lancelot, C., Likens, G.E., 2009. Controlling eutrophication: nitrogen and phosphorus. Science 323, 1014–1015.

Coops, H., Beklioglu, M., Crisman, T.L., 2003. The role of water-level fluctuations in shallow lake ecosystems–workshop conclusions. Hydrobiologia 506, 23–27.

Cotner, J.B., 2017. Nitrogen is not a house of cards. Environ. Sci. Technol. 51, 3. -3.

Derrien, M., Brogi, S.R., Gonçalves-Araujo, R., 2019. Characterization of aquatic organic matter: assessment, perspectives and research priorities. Water Res. 163, 114908.

Diaz, R.J., Rosenberg, R., 2008. Spreading dead zones and consequences for marine ecosystems. Science 321, 926–929.

Dierberg, F.E., DeBusk, T.A., Jackson, S.D., Chimney, M.J., Pietro, K., 2002. Submerged aquatic vegetation-based treatment wetlands for removing phosphorus from agricultural runoff: response to hydraulic and nutrient loading. Water Res. 36, 1409–1422.

Dong, B., Han, R., Wang, G., Cao, X., 2014. O_2, pH, and redox potential microprofiles around Potamogeton malaianus measured using microsensors. PLoS ONE 9, e101825.

Duan, H., Loiselle, S.A., Zhu, L., Feng, L., Zhang, Y., Ma, R., 2015. Distribution and incidence of algal blooms in Lake Taihu. Aquat. Sci. 77, 9–16.

Gibbons, K.J., Bridgeman, T.B., 2020. Effect of temperature on phosphorus flux from anoxic western Lake Erie sediments. Water Res. 182, 116022.

Gu, S., Gruau, G., Dupas, R., Petitjean, P., Li, Q., Pinay, G., 2019. Respective roles of Fe-oxyhydroxide dissolution, pH changes and sediment inputs in dissolved phosphorus release from wetland soils under anoxic conditions. Geoderma 338, 365–374.

Han, C., Ren, J., Wang, Z., Yang, S., Ke, F., Xu, D., Xie, X., 2018. Characterization of phosphorus availability in response to radial oxygen losses in the rhizosphere of Vallisneria spiralis. Chemosphere 208, 740–748.

Ho, J.C., Michalak, A.M., Pahlevan, N., 2019. Widespread global increase in intense lake phytoplankton blooms since the 1980s. Nature 574, 667–670.

Hupfer, M., Lewandowski, J., 2008. Oxygen Controls the Phosphorus Release from Lake Sediments–a Long-Lasting Paradigm in Limnology. Int. Rev. Hydrobiol. 93, 415–432.

Jensen, H.S., Kristensen, P., Jeppesen, E., Skytthe, A., 1992. Iron: phosphorus ratio in surface sediment as an indicator of phosphate release from aerobic sediments in shallow lakes. Hydrobiologia 235, 731–743.

Ji, N., Liu, Y., Wang, S., Wu, Z., Li, H., 2022. Buffering effect of suspended particulate matter on phosphorus cycling during transport from rivers to lakes. Water Res. 216, 118350.

Kim, B., Choi, A., Lee, K.-S., Kang, C.-K., Hyun, J.-H., 2017. Sulfate Reduction and Sulfur Cycles at Two Seagrass Beds Inhabited by Cold Affinity Zostera marina and Warm Affinity Halophila nipponica in Temperate Coastal Waters. Estuar Coasts 40, 1346–1357.

Kisand, A., Nõges, P., 2003. Sediment phosphorus release in phytoplankton dominated versus macrophyte dominated shallow lakes: importance of oxygen conditions. Hydrobiologia 506, 129–133.

Kong, M., Liu, C., Chao, J., Wang, L., Gao, Y., Peng, F., Xu, X., Han, T., Wang, P., Wang, C., 2020. Field observation and simulation experiments on nutrient transformation during phytoplankton-derived particulate matter deposition. Environ. Sci. Pollut. Res. 27, 25297–25311.

Koop-Jakobsen, K., Fischer, J., Wenzhöfer, F., 2017. Survey of sediment oxygenation in rhizospheres of the saltmarsh grass-Spartina anglica. Sci. Total Environ. 589, 191–199.

Lehtoranta, J., Ekholm, P., Pitkänen, H., 2009. Coastal eutrophication thresholds: a matter of sediment microbial processes. AMBIO A J. Hum. Environ. 38, 303–308.

Li, J., Zhang, Y., Katsev, S., 2018. Phosphorus recycling in deeply oxygenated sediments in Lake Superior controlled by organic matter mineralization. Limnol. Oceanogr. 63, 1372–1385.

Liu, C., Du, Y., Yin, H., Fan, C., Chen, K., Zhong, J., Gu, X., 2019a. Exchanges of nitrogen and phosphorus across the sediment-water interface influenced by the external suspended particulate matter and the residual matter after dredging. Environ. Pollut. 246, 207–216.

Liu, C., Shao, S., Zhang, L., Du, Y., Chen, K., Fan, C., Yu, Y., 2019b. Sulfur development in the water-sediment system of the algae accumulation embay area in Lake Taihu. Water (Basel) 11, 1817.

Liu, C., Shen, Q., Zhou, Q., Fan, C., Shao, S., 2015. Precontrol of algae-induced black blooms through sediment dredging at appropriate depth in a typical eutrophic shallow lake. Ecol. Eng. 77, 139–145.

Lukkari, K., Hartikainen, H., Leivuori, M., 2007. Fractionation of sediment phosphorus revisited. I: fractionation steps and their biogeochemical basis. Limnol. Oceanogr. Methods 5, 433–444.

Markovic, S., Liang, A., Watson, S.B., Guo, J., Mugalingam, S., Arhonditsis, G., Morley, A., Dittrich, M., 2019. Biogeochemical mechanisms controlling phosphorus diagenesis and internal loading in a remediated hard water eutrophic embayment. Chem. Geol. 514, 122–137.

Nürnberg, G.K., Tarvainen, M., Ventelä, A.-.M., Sarvala, J., 2012. Internal phosphorus load estimation during biomanipulation in a large polymictic and mesotrophic lake. Inland Waters 2, 147–162.

Pełechaty, M., Pukacz, A., Apolinarska, K., Pełechata, A., Siepak, M.J.S., 2013. The significance of Chara vegetation in the precipitation of lacustrine calcium carbonate. Sedimentology 60, 1017–1035.

Qin, B., Paerl, H.W., Brookes, J.D., Liu, J., Jeppesen, E., Zhu, G., Zhang, Y., Xu, H., Shi, K., Deng, J., 2019. Why Lake Taihu continues to be plagued with cyanobacterial blooms through 10 years (2007-2017) efforts. Sci. Bull. 64, 354–356.

Qin, B., Zhou, J., Elser, J.J., Gardner, W.S., Deng, J., Brookes, J.D., 2020. Water depth underpins the relative role and fates of nitrogen and phosphorus in lakes. Environ. Sci. Technol. 54, 3191–3198.

Rasmussen, H., Jorgensen, B.B., 1992. Microelectrode studies on seasonal oxygen uptake in a coastal sediment: role of molecular diffusion. Mar. Ecol. Progress 81, 289–303.

Rönicke, H., Frassl, M.A., Rinke, K., Tittel, J., Beyer, M., Kormann, B., Gohr, F., Schultze, M., 2021. Suppression of bloom-forming colonial cyanobacteria by phosphate precipitation: a 30 years case study in Lake Barleber (Germany). Ecol. Eng. 162, 106171.

Rozan, T.F., Taillefert, M., Trouwborst, R.E., Glazer, B.T., Ma, S., Herszage, J., Valdes, L. M., Price, K.S., Luther III, G.W., 2002. Iron-sulfur-phosphorus cycling in the sediments of a shallow coastal bay: implications for sediment nutrient release and benthic macroalgal blooms. Limnol. Oceanogr. 47, 1346–1354.

Rydin, E., 2000. Potentially mobile phosphorus in Lake Erken sediment. Water Res. 34, 2037–2042.

Sand-Jensen, K., Martinsen, K.T., Jakobsen, A.L., Sø, J.S., Madsen-Østerbye, M., Kjær, J. E., Kristensen, E., Kragh, T., 2021. Large pools and fluxes of carbon, calcium and phosphorus in dense charophyte stands in ponds. Sci. Total Environ. 765, 142792.

Scheffer, M., Van Nes, E.H., 2007. Shallow lakes theory revisited: various alternative regimes driven by climate, nutrients, depth and lake size. Hydrobiologia 584, 455–466.

Schindler, D.W., Carpenter, S.R., Chapra, S.C., Hecky, R.E., Orihel, D.M., 2016. Reducing phosphorus to curb lake eutrophication is a success. Environ. Sci. Technol. 50, 8923–8929.

Shen, Q., Zhou, Q., Shang, J., Shao, S., Zhang, L., Fan, C., 2014. Beyond hypoxia: occurrence and characteristics of black blooms due to the decomposition of the submerged plant Potamogeton crispus in a shallow lake. J. Environ. Sci. 26, 281–288.

Shinohara, R., Imai, A., Kohzu, A., Tomioka, N., Furusato, E., Satou, T., Sano, T., Komatsu, K., Miura, S., Shimotori, K., 2016. Dynamics of particulate phosphorus in a shallow eutrophic lake. Sci. Total Environ. 563, 413–423.

Søndergaard, M., Jensen, J.P., Jeppesen, E., 2003. Role of sediment and internal loading of phosphorus in shallow lakes. Hydrobiologia 506, 135–145.

Song, C., Cao, X., Zhou, Y., Azzaro, M., Monticelli, L.S., Leonardi, M., La Ferla, R., Caruso, G., 2018. Different pathways of nitrogen and phosphorus regeneration mediated by extracellular enzymes in temperate lakes under various trophic state. Environ. Sci. Pollut. Res. 25, 31603–31615.

Taguchi, V.J., Olsen, T.A., Natarajan, P., Janke, B.D., Gulliver, J.S., Finlay, J.C., Stefan, H.G., 2020. Internal loading in stormwater ponds as a phosphorus source to downstream waters. Limnol. Oceanogr. Lett. 5, 322–330.

Tammeorg, O., Nürnberg, G., Horppila, J., Haldna, M., Niemistö, J., 2020. Redox-related release of phosphorus from sediments in large and shallow Lake Peipsi: evidence from sediment studies and long-term monitoring data. J. Great Lakes Res. 46, 1595–1603.

Ullman, W.J., Aller, R.C., 1982. Diffusion coefficients in nearshore marine sediments. Limnol. Oceanogr. 27, 552–556.

Wang, L., Song, H., Wu, X., An, J., Wu, Y., Wang, Y., Li, B., Liu, Q., Dong, B., 2022. Relationship between the coprecipitation of phosphorus-on-calcite by submerged macrophytes and the phosphorus cycle in water. J. Environ. Manag. 314, 115110.

Yang, P., Yang, C., Yin, H., 2020. Dynamics of phosphorus composition in suspended particulate matter from a turbid eutrophic shallow lake (Lake Chaohu, China): implications for phosphorus cycling and management. Sci. Total Environ. 741, 140203.

Yin, H., Ren, C., Li, W., 2018. Introducing hydrate aluminum into porous thermally-treated calcium-rich attapulgite to enhance its phosphorus sorption capacity for sediment internal loading management. Chem. Eng. J. 348, 704–712.

Zhang, Q., Dong, X., Yang, X., Liu, E., Lin, Q., Cheng, L., Liu, L., Jeppesen, E., 2022. Aquatic macrophyte fluctuations since the 1900s in the third largest Chinese freshwater lake (Lake Taihu): evidences, drivers and management implications. Catena 213, 106153.

Zhang, Y., Jeppesen, E., Liu, X., Qin, B., Shi, K., Zhou, Y., Thomaz, S.M., Deng, J., 2017. Global loss of aquatic vegetation in lakes. Earth-Sci. Rev. 173, 259–265.

Zhao, Y., Zhang, Z., Wang, G., Li, X., Ma, J., Chen, S., Deng, H., Annalisa, O.-.H., 2019. High sulfide production induced by algae decomposition and its potential stimulation to phosphorus mobility in sediment. Sci. Total Environ. 650, 163–172.

Zhu, G., Zou, W., Guo, C., Qin, B., Zhang, Y., Xu, H., Zhu, M., 2020. Long-term variations of phosphorus concentration and capacity in Lake Taihu, 2005–2018: implications for future phosphorus reduction target management. J. Lake Sci. 32, 21–35.